Automatic Measurement of Inner Ear in Different Mammals[1]

Yi Du[1,#], Han-dai Qin[1,#], Chen Liu[1,#] , Da Liu[1,#] , Shuo-long Yuan[1], Qing-qing Jiang[1], Jun Yang[2], Gang Li[3], Hong-lan Xie[4], Jian-guo Zhao[2], Ning Yu[1,*] and Shi-ming Yang[1,*]

1. Department of Otolaryngology, Head and Neck Surgery, Institute of Otolaryngology, Department of Radiology, Chinese PLA General Hospital, Beijing, China;

2. Institute of Zoology, Chinese Academy of Sciences, Beijing, China;

3. Institute of Material Medical, Chinese Academy of Medical Sciences and Peking Union Medical College, Beijing, China;

4. Shanghai Institute of Applied Physics, Chinese Academy of Sciences, Shanghai, China.

Abstract：***Objective:*** The aim of this research is to develop an accurate and automatic measuring method based on the aid of centerline to construct three dimensional models of inner ear in different mammals and to assess the morphological variations. ***Methods:*** Three adult healthy mice, three adult guinea pigs, three adult mini pigs and one left temporal bone of human were included in this research. All 18 animal specimens and the human sample were scanned with the use of Micro-CT. After being segmented, three-dimensional models of the inner ear in different mammals were reconstructed using Mimics. A novel method with the use of centerline was established to estimate the properties of 3D models and to calculate the length, volume and angle parameters automatically. ***Results:*** Morphological models of inner ears in different mammals have been built, which describe detailed shape of cochlear, vestibule, semicircular canals and common crus. Mean value of lengths and volumes of the cochlear, lateral semicircular canal, superior semicircular canal and posterior semicircular canal, tended to increase with the body size of the mammals, showed the proximity to the human data in mini pig. The angles between the semicircular canal planes showed differences between mammals. The mean values of semicircular canals of mice and mini pigs closely resembled to human data in numerical assessment. ***Conclusion:*** The automatic measurement of the inner ear based on centerline builds an effective way to assess lengths, volumes and angles of three-dimensional structures. This study provides a theoretical basis for mechanical analysis of inner ear in different mammals and proves the similarity between mini pig and human.

Key words: Automatic measurement, centerline, inner ear structures, 3D model, hearing loss, animal model, mechanical analysis

---

[1] This study was supported by national key research and development plan (2020YFC2004002) and Noise Research Fund (No. BWS14B080 and JDZYY20132)

# Yi Du, Han-dai Qin, Chen Liu and Da Liu contributed equally to this work

* Corresponding author Shiming Yang or Ning Yu, Department of Otolaryngology, Head and Neck Surgery, Institute of Otolaryngology, Chinese PLA General Hospital, 28 Fuxing Road, Beijing 100853, P. R. China. E-mail: yangsm301@263.net or yuning@301hospital.org

Automatic Measurement of Inner Ear in Different Mammals

1. Introduction

The osseous labyrinth, located in the petrous portion of the temporal bone, consists of the vestibule, semicircular canals, and cochlea. All these small and irregular inner ear components and their inter space relationships are vital in both surgical procedures and basic studies [1-3]. The fine and intricate geometric characteristic of the inner ear needs a deeper insight into the structure. Image scanning has been the perfect method for such purpose. Thereby, a variety of techniques have been used to acquire topography images, such as traditional histology sectioning, computed tomography (CT), magnetic resonance imaging (MRI) and synchrotron radiation-based micro computed tomography [1, 4-8]. With the development of post-processing and computer visualization, observation and calculation of solid objects become a reality. Those 3D models rotating in arbitrary angles help to fully grasp anatomy features, discover fine structure variations and improve the ability to evaluate pathologic conditions [3, 8, 9]. Considering density resolution and operation procedures, CT seems to be the optimal method to obtain inner ear topography [3, 4, 8-10]. Micro-CT is a variation of CT with a higher resolution and, hence, could meet the requirement of remodeling fine inner ear structures [4, 11].

Lower mammals play an important role in biomedical research of otology, for instance, visualize the temporal bone, evaluate the surgical trauma and build hearing loss model [1-6, 8-10, 12-15]. Accurate measurement of length, volume and shape of the solid object of inner ear benefits mechanical modeling and stress analysis[16, 29]. Fully understanding of the morphology of these animal models would allow further biomechanical development on inner ear [11, 14, 17]. However, quantitative analysis of these different 3D models depends highly on elaborate preparation, image resolution and iterative measurements, which may cause radiation damage or inevitable error and eventually affect accuracy and validity of results [1, 8, 9]. Apart

from that, there are few researches on the quantitative analysis of inner ear between different mammals, thus the application of animal models is limited.

Although the inner ear structure is complicated, the cochlear is very close to a spiral shape and the semicircular canals are close to circles. Recently, the centerline method, successfully used in the segmentation of the vessel[18], vocal tract[19, 20] and cochlear[12], shows good properties in path tracking, which make it possible to describe the feature of intricate solid objects like inner ear.

Accordingly, this article tries to overcome the above inadequacies of traditional 3D imaging with the use of centerlines, which focused on different mammal inner ear models and can describe the feature parameters automatically. This provides an advanced method which could be widely used in structural and parametric researches. The present study provides a comprehensive visualization of inner ear in different animal models as well as in human and describes the discrepancies between animal models and human labyrinth mathematically.

2. Materials and Methods

2.1 Preparation of mammal specimens

To investigate the differences between animals, adult healthy mice, guinea pigs and mini pigs (n=3 in each group) were included in this research. To compare the variations between animals and human, a left human temporal bone without any evidence of malformation was analyzed. The study was conducted with approval of the Institutional Animal Care and Use Committee of General Hospital of PLA.

For getting an image of intact inner ear, the animal samples were prepared as follows. After an intraperitoneal injection of a lethal dose of sodium pentobarbital, mice, guinea pigs and mini pigs were sacrificed. Following decapitation, the heads of the mice and the guinea pigs were divided and both their left and right bullaes were removed for image acquisition. The left and right temporal bones of mini pigs were cut right after decapitation, including the complete middle and inner ear. All the specimens were immediately scanned after above steps. Iterative procedures for sample preparation, unavoidably leading to shrinkage in the samples [8], are not necessary to our study which primarily aimed at testing the efficiency of a novel

measuring method. Therefore, no steps of fixation, dehydration and decalcification were processed in our research.

2.2 Micro-CT scanning procedure

All the prepared samples were scanned using a high-speed Micro-CT system (PerkinElmer Inc., Norwalk, CT, USA). A 5×5mm field of view was used in the samples of mice, 20×20mm field of view in guinea pigs and mini pigs, 30×30mm field of view in human temporal bone. The scan was performed at a voltage of 90 kV and a current of 120 μA. A fast scan time of 4.5min was set and 512 slices of image with voxel size of 9μm, 39μm and 59μm were achieved in these cases. Data set was exported to disc in the type of DICOM after the process of workstation. No defects or infections were showed in all three samples.

2.3 3D reconstruction

Then MIMICS (Materialises interactive medical image control system, Belgium) was used in this research to process the images and reconstruct 3D volume. The function of interpolation in the MIMICS allows semi-automated segment between the slices [4]. Firstly, the segmentation was achieved automatically using different gray values, which can separate the object from the background. To remove artifacts not belong to the object, manual segmentation was supplemented to fit the target region. The segmentation results were checked and adjusted in transversal and coronal planes as well as 3D views.

After defining the mask in involving slices, the region of interest was determined. Then calculate the mask, 3D volume of labyrinth embedded in the temporal bone was rendered (Fig.1). Further smooth and modification were carried on for the purpose of calculation.

Fig. 1 Volume render of the left temporal bone and inner ear in mini pig model. The temporal bone is rendered translucent.

2.4 Automatic Measurements of 3D models

2.4.1 Calculate Centerline

Fit centerline, one of the Medcad modules in Mimics, was used to automatically calculate the centerlines of 3D models. After finishing centerline calculation, control points could be easily added if necessary. The centerlines and nodes of models were illustrated in Fig.2 and Fig.3.

Fig. 2 Centerlines in 3D model of inner ear in mini pig

Fig. 3 Centerlines and nodes of inner ear in mini pig

2.4.2 Automatic measurements of inner ear parameters in various samples

The unique nodes in the centerlines were used as landmarks. The landmarks in the 3D models were mapped to corresponding anatomic locations in inner ear. The distances between the landmarks were used to calculate the length automatically. The length of the cochlea was automatically measured from the landmark of apex of the cochlea to the round window niche (fiburcation) through the centerline. The length of anterior and posterior semicircular canal were measured from the feature points representing ampulla to common crus. The length of lateral semicircular canal was measured between two foot points. The common crus length was also measured by two foot points.

Based on the landmarks, the 3D model of the labyrinth was segmented into six parts, cochlea (CO), vestibule (VL), anterior semicircular canal (ASC), lateral semicircular canal (LSC), posterior semicircular canal (PSC) and common crus (CC). Then, the volumes of these six components were computed automatically in Mimics software.

The centerlines was exported in the form of IGS and imported into a geometry

reconstruction software Geomagic Studio (Geomagic, Morrisville, North Carolina, USA) for further analysis. Reference plane in corresponding semicircular canals was defined with the use of plane of best fit in feature modules (shown in Fig.4). Take the anterior SC and lateral SC as an example, shown in Fig. 5, the method of obtaining the plane included angle is as follows: $\vec{a} = (a1, a2, a3)$ is the vector of the anterior SC reference plane; $\vec{b} = (b1, b2, b3)$ is the vector of the lateral SC reference plane; the angle between the two intersection plane is described in Eq.(1).

$$\cos\alpha = \frac{\vec{a} \cdot \vec{b}}{|\vec{a}||\vec{b}|}$$

Eq. (1)

The algorithm to calculate the angles was realized through Matlab platform (MATHWORKS INC, Natic, USA).

Fig. 4 Illustration of the best fit plane in mini pig model, ASC is the reference plane of anterior semicircular canal, LSC is the reference plane of lateral semicircular canal, PSC is the reference plane of posterior semicircular canal

Fig. 5 Illustration of the angle measurement in mini pig model, a: axis of the plane of the anterior semicircular canal; b: axis of the plane of the lateral semicircular canal; α: included angle between a and b

3. Results

3.1 Geometric reconstruction of inner ear renders exquisite structures of CO, VL and SC

The intricate, elaborate structure of inner ear model was rendered as a complex geometric solid comprising of cochlea, vestibule and semicircular canals, shown in Fig. 6. The 3D visualization made it possible to observe the surface texture and anatomical details of the inner ear, such as the apical and basal turn as well as the round window and oval window. The spatial location and concrete form of the semicircular canals clearly embodied in 3D models. Three similar-circular canals owned similar lengths and was visually perpendicular to each other. Common crus

and ampulla were also easy to recognize from the models. To our knowledge, the detailed 3D visualization of the mini pig inner ear in our research is shown for the first time.

Fig. 6 Illustration of inner ear structure of different mammals.(A: mouse; B: guinea pig; C: mini pig; D: human) CO-cochlea; VL-vestibule; LSC-lateral semicircular canal; ASC-anterior semicircular canal; PSC-posterior semicircular canal; CC-common crus

3.2 The length parameters of inner ear increases with body size of mammals

Fig. 7 showed the morphology of centerlines and landmarks in three animal models and human model. The centerlines and landmarks formed a framework of a brief characteristic description of inner ears. Characteristics in centerlines mapped to the morphological features of three-dimensional models, such as oval window, ampulla and common crus. The turns of the cochlear varied among animals, specifically mouse is 2 turns, guinea pig is 4 turns and 3.5 turns for the mini pig, but the human cochlear is less than 3 turns(Fig.8).

Fig. 7 Centerlines and landmarks in various mammal models.(A,B: mouse inner ear model(A) and its centerlines and landmarks(B); C,D: guinea pig inner ear model(C) and its centerlines and landmarks(D); E,F: mini pig inner ear model(E) and its centerline and landmarks(F); G,H: human inner ear model(G) and its centerline and landmarks(H)

The length measurements of inner ear models were listed in Table 1, including cochlea, lateral semicircular canal, anterior semicircular canal, posterior semicircular canal and common crus. Among all the measurements, cochlear length was the maximum distance. The lengths of three semicircular canals were similar to each other. Lengths increased with body size, and among them the mean value of cochlear

length of mini pigs were the closest to human.

Fig. 8 Cochlear turns of different mammals (A: mouse cochlear; B: guinea pig cochlear; C: pig cochlear; D: human cochlear)

Table 1. Length Measurements of Inner Ear

3.3 The volume parameters of the inner ear increases with body size of animals

Fig. 6 illustrated the 3D model of different animal inner ears with segmented and color-marked components: cochlea (yellow), vestibule (green), anterior semicircular canal (red), lateral semicircular canal (gray), posterior semicircular canal (blue) and common crus (purple), the volume of each part was calculated automatically in Mimics. Generally, the inner ear volume of mice, Guinea pigs and mini pigs were less than that of human and increased with the body size. In each experimental animal, the largest portion was cochlea, the next is vestibule, then is three semicircular canals and the least is common crus. Detailed data was shown in Table 2.

Table 2. Volume Measurements of Inner Ear

3.4 The angle parameters of mini pig inner ear are closest to human inner ear

Spatial relationship between the semicircular canals were illustrated in Table 3(the angle parameters of mice, guinea pigs and mini pigs were shown in Mean±SD). The three reference planes are mutually perpendicular in vision, whereas the angle parameter were differ from each other. Our research also compared the angle discrepancy between experimental animal models and human data with the use of Euclidean distance. The detailed distance was calculated by Eq. (2).

$$Distance_{ani} = \sqrt{(LA_{ani} - LA_{hum})^2 + (LP_{ani} - LP_{hum})^2 + (AP_{ani} - AP_{hum})^2}$$

Eq. (2)

The $Distance_{ani}$ is the Euclidean distance between each animal and human, LA is

the angle between lateral and anterior semicircular canal reference planes, LP is the angle between lateral and posterior semicircular canal reference planes, AP is the angle between anterior and posterior semicircular canal reference planes, ani represents angle parameter in each animal (mice, guinea pigs and mini pigs) and hum is the angle data in human. The results of Euclidean distance indicated that the angle parameters of mice are closest to human in measurements, the mini pigs are also very similar, the least is guinea pigs, namely, spatial relationship of semicircular canals was more approximate to human in mice and mini pigs than that in guinea pigs.

Table 3. Angle Measurements between the Semicircular Canals

4. Discussion

Inner ear morphological differences between different mammal models were described in this study. To our knowledge, this is the first study on the 3D visualization and precise measurements of inner ear in mini pig model. All length, volume and angle parameters of inner ear in mini pigs were more similar to human in numerical value than mice or Guinea pigs which were widely used in the research on hearing loss. Former verdicts about the mini pig middle ear similarity to human had been fully verified [21, 22] and those studies had also explored evaluation of mini pig cochlear. Due to different measuring method and animal samples, the above literatures had described that the length of mini pig cochlear was approximately 39.48mm coiling three and a half times which was larger than our current research(mean value is 26.09mm). The mean length of mice cochlear in our measurement was 6.14mm, approaching to previous data ranging from 5.81mm to 6.67mm [5, 23, 24]. Our data of mice cochlear volume of 1.54mm^3 was resembled to Buytaert's result (1.702mm^3) [8]. As to the guinea pig cochlear, the mean length was 17.65mm which was consistent with other researches ranging from 15.7mm to 22mm [14, 25]. Due to different imaging acquisition and measuring method, volume and length of human inner ear were slightly underestimated in our research compared to previous data [1, 4, 7, 9, 26]. Melhem et al. reported the volumetric

measurements of female human inner ear range from 172.3mm^3 to 241.9mm^3, indicating that there are some variabilities in length and volume of inner ear between individuals [7].

The semicircular canals are sensory organs which are sensitive to angular accelerations of the head [27]. The understanding of planer orientation of semicircular canals is important to investigate compensatory eye movements due to vestibule-ocular reflex which occurs parallel to the plane of each semicircular canal, that is the basis for test and treatment for dizzy patient[27, 28]. Although three semicircular canals were perpendicular to each other visually, the plane included angles were different in precise measurements. With the method of histologic section, Hashimoto et al. reconstructed the 3D models of semicircular canals of 7 human temporal bones and reported the average angle for each pair of semicircular canals is approximately 90°[27]. Aoki et al. investigated 11 persons with intact vestibular function with MR scan, and reported that the average of L-A SC is 91.6°, L-P SC is 90.8° and A-P SC is 96.2° [28]. Christensen et al. studied 10 human data set, and calculated the average of L-A SC is 92.79°, L-P SC is 90.93°, A-P SC is 100.75° [1]. Our result of human model shows a little difference with previous data due to different measuring method. Former angle measurements were commonly based on manual process [1, 28] and complicated equations [7], that would cause inevitable error and influence data accuracy. Besides, this research made the first comparison of plane included angles of semicircular canals in different mammals, suggesting the mini pig and mouse are similar to human in angle assessments. With the help of centerlines and landmarks, it is easy to define the reference plane of semicircular canal and calculate the angle parameters automatically.

However, there are some potential limitations and research directions that should be taken into consideration. Firstly, the fundamental issue about reconstruction is the image resolution and could also be effected by the field of view, object size and orientation[8], which should be improved in further research. Because of the relatively lower resolution, supplementary modification is necessary in the procedure of reconstruction, which might overestimate the volume parameters by incorporating vessels, fluid and other soft tissues in the gaps [8]. Secondly, for the

purpose of proposing an automatic measuring method suitable for different animals, only three animals (6 samples) in each species was included in this article. Interspecific comparisons and bilateral variations should be taken into analysis. Moreover, morphological changes like shrinkage induced by the process of fixation, decalcification and dehydration [8, 29], not necessary to micro-CT scan, were avoided in our preparation procedures, which could influence the image quality. Based on higher resolution of imaging, further reconstructions and measurements will be focused on the detailed anatomical inner ear structure like vestibular aqueduct, internal acoustic meatus and endolymphatic sac which had been indicated firmly related to hearing loss.

In summary, an automatic measuring method for inner ear based on centerlines was proposed in this research. With this method, we were able to describe the morphologic characters of inner ear in different mammals, among which mini pig model is most similar to human according to quantitative length, volume and angle measurements. This method is helpful to understand the morphological characteristics of inner ear in different mammals and the knowledge of animal models may find a border application in pathological diagnosis and biomedical analysis in the future.

Reference

[1] Christensen G E, He J, Dill J A, et al. Automatic measurement of the labyrinth using image registration and a deformable inner ear atlas[J]. Academic Radiology. 2003, 10(9): 988-999.

[2] Du Yi, Ren Li-Li, Jiang Qing-Qing, et al. Degeneration of saccular hair cells caused by MITF gene mutation [J]. Neural Dev. 2019 Jan 11;14(1):1. doi: 10.1186/s13064-019-0126-0.

[3] Skrzat J, Wróbel A, Walocha J. A preliminary study of three-dimensional reconstruction of the human osseous labyrinth from micro-computed tomography scans[J]. Folia Morphologica. 2013, 72(1): 17-21.

[4] Avci E, Nauwelaers T, Lenarz T, et al. Variations in microanatomy of the human cochlea[J]. Journal of Comparative Neurology. 2014, 522(14): 3245-3261.

[5] Rau C, Hwang M, Lee W K, et al. Quantitative X-ray tomography of the mouse cochlea[J]. PLoS One. 2012, 7(4): e33568.

[6] Muller M, von Hunerbein K, Hoidis S, et al. A physiological place-frequency map of the cochlea in the CBA/J mouse[J]. Hear Res. 2005, 202(1-2): 63-73.

[7] Melhem E R, Shakir H, Bakthavachalam S, et al. Inner ear volumetric measurements using high-resolution 3D T2-weighted fast spin-echo MR imaging: initial experience in healthy subjects[J]. AJNR Am J Neuroradiol. 1998, 19(10): 1819-1822.

[8] Buytaert J A N, Johnson S B, Dierick M, et al. MicroCT versus sTSLIM 3D Imaging of the Mouse Cochlea[J]. Journal of Histochemistry & Cytochemistry. 2013, 61(5): 382-395.

[9] Shin K J, Lee J Y, Kim J N, et al. Quantitative analysis of the cochlea using three-dimensional reconstruction based on microcomputed tomographic images[J]. Anat Rec (Hoboken). 2013, 296(7): 1083-1088.

[10] Buytaert J A N, Salih W H M, Dierick M, et al. Realistic 3D Computer Model of the Gerbil Middle Ear, Featuring Accurate Morphology of Bone and Soft Tissue Structures[J]. Journal of the Association for Research in Otolaryngology. 2011, 12(6): 681-696.

[11] Poznyakovskiy A A, Zahnert T, Kalaidzidis Y, et al. The creation of geometric three-dimensional models of the inner ear based on micro computer tomography data[J]. Hearing Research. 2008, 243(1-2): 95-104.

[12] Poznyakovskiy A A, Zahnert T, Kalaidzidis Y, et al. A segmentation method to obtain a complete geometry model of the hearing organ[J]. Hearing Research. 2011, 282(1-2): 25-34.

[13] Honda K, Noguchi Y, Kawashima Y, et al. Ex vivo visualization of the mouse otoconial layer compared with micro-computed tomography[J]. Otol Neurotol. 2015, 36(2): 311-317.

[14] Lee C F, Li G J, Wan S Y, et al. Registration of micro-computed tomography and histological images of the guinea pig cochlea to construct an ear model using an iterative closest point algorithm[J]. Ann Biomed Eng. 2010, 38(5): 1719-1727.

[15] Eacute E, Bernard, James C, et al. The Size of the Cochlea and Predictions of Insertion Depth Angles for Cochlear Implant Electrodes[J]. Audiology and Neurotology. 2006, 11(1): 27-33.

[16] Higashimachi T, Toriya R, Suga K. Finite Element Analysis of External, Middle and Inner Ear under Loads through Temporomandibular Joint[J]. Key Engineering Materials. 2012, 516: 457-462.

[17] Ifediba M A, Rajguru S M, Hullar T E, et al. The role of 3-canal biomechanics in angular motion transduction by the human vestibular labyrinth[J]. Ann Biomed Eng. 2007, 35(7): 1247-1263.

[18] Lesage D, Angelini E D, Bloch I, et al. A review of 3D vessel lumen segmentation techniques: Models, features and extraction schemes[J]. Medical Image Analysis. 2009, 13(6): 819-845.

[19] Poznyakovskiy A A, Mainka A, Platzek I, et al. A Fast Semiautomatic Algorithm for Centerline-Based Vocal Tract Segmentation[J]. BioMed Research International. 2015, 2015: 1-7.

[20] Mainka A, Poznyakovskiy A, Platzek I, et al. Lower Vocal Tract Morphologic Adjustments Are Relevant for Voice Timbre in Singing[J]. PLOS ONE. 2015, 10(7): e132241.

[21] Yi H J, Guo W, Wu N, et al. The temporal bone microdissection of miniature pigs as a useful large animal model for otologic research[J]. Acta Otolaryngol. 2014, 134(1): 26-33.

[22] Yi H, Guo W, Chen L, et al. Microdissection of miniature pig ear[J]. Journal of Otology. 2013(02): 91-96.

[23] Susan Keiler C R. Cochlear dimensions obtained in hemicochleae of four dijerent strains of mice: CBA/CaJ, 129/CD1, 129/SvEv and C57BL/6J[J]. Hearing research. 2001, 1-2(162): 91-104.

[24] Burda H, Branis M. Postnatal development of the organ of Corti in the wild house mouse, laboratory mouse, and their hybrid[J]. Hear Res. 1988, 36(1): 97-105.

[25] Salt A N, Henson M M, Gewalt S L, et al. Detection and quantification of endolymphatic hydrops in the guinea pig cochlea by magnetic resonance microscopy[J]. Hear Res. 1995, 88(1-2): 79-86.

[26] Ketten D R, Skinner M W, Wang G, et al. In vivo measures of cochlear length and insertion depth of nucleus cochlear implant electrode arrays[J]. Ann Otol Rhinol Laryngol Suppl. 1998, 175: 1-16.

[27] Hashimoto S, Naganuma H, Tokumasu K, et al. Three-dimensional reconstruction of the human semicircular canals and measurement of each membranous canal plane defined by Reid's stereotactic

coordinates[J]. Ann Otol Rhinol Laryngol. 2005, 114(12): 934-938.
[28] Aoki S, Takei Y, Suzuki K, et al. Planer orientation of the bilateral semicircular canals in dizzy patients[J]. Auris Nasus Larynx. 2012, 39(5): 451-454.
[29] Caiqin Wu L Y P D. Three-dimensional Models of the Membranous Vestibular Labyrinth in the Guinea Pig Inner Ear: 4th International Conference on Biomedical Engineering and Informatics (BMEI) [Z]. 2011.

Fig. 1

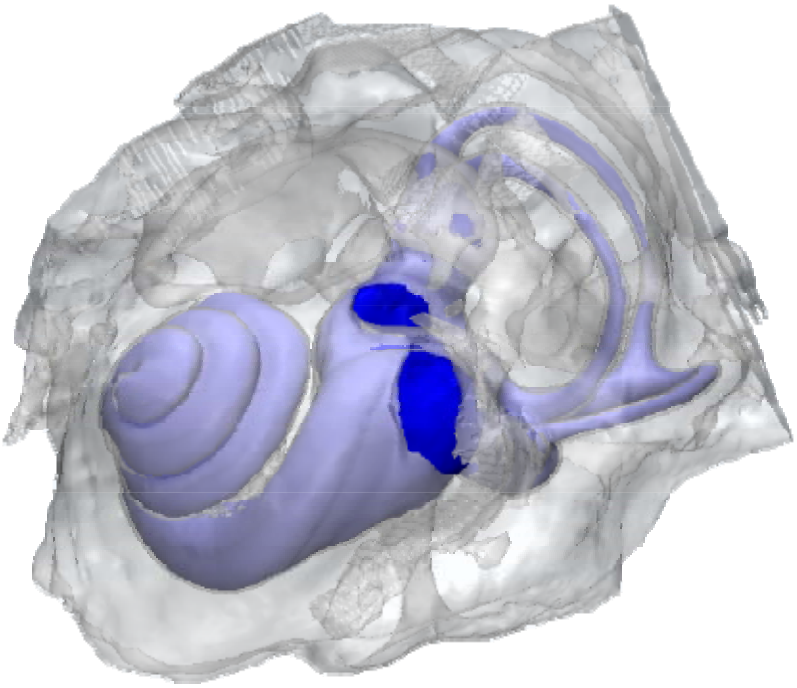

Fig. 1 Volume render of the left temporal bone and inner ear in mini pig model. The temporal bone is rendered translucent.

Fig. 2

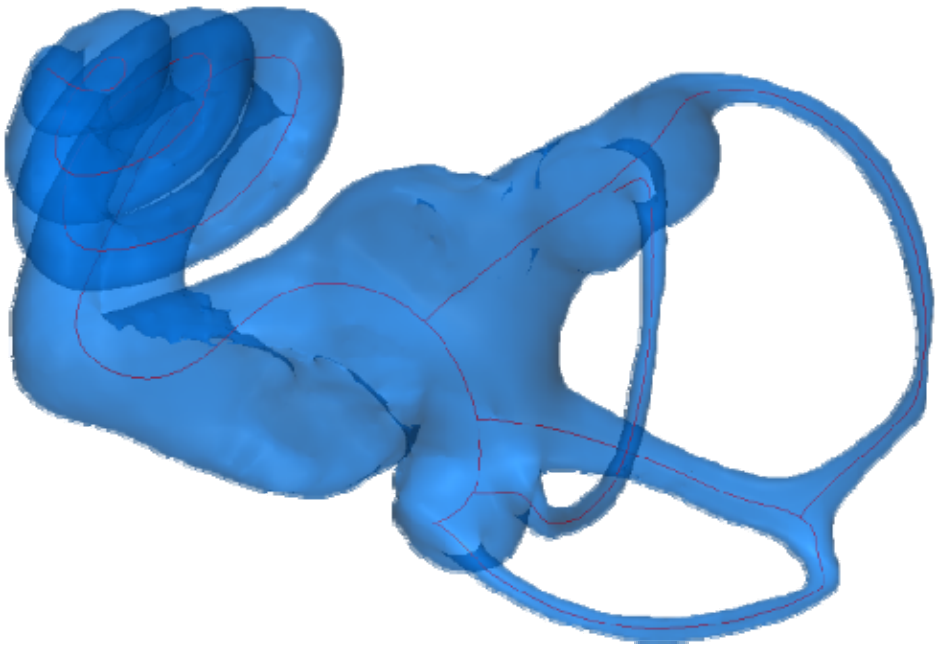

Fig. 2 Centerlines in 3D model of inner ear in mini pig

Fig. 3

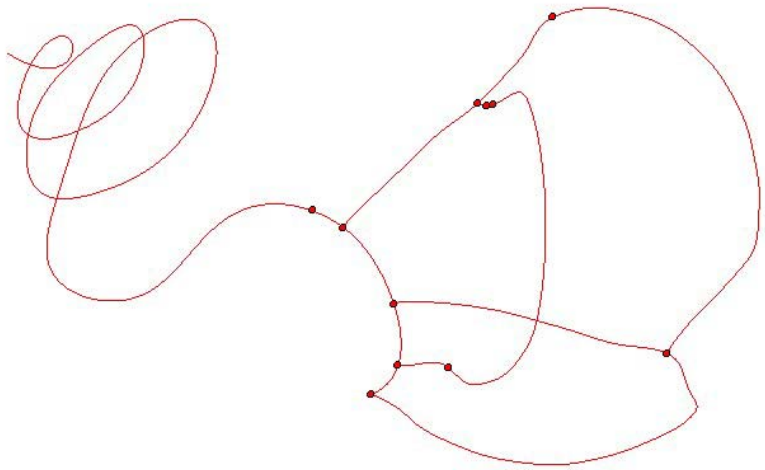

Fig. 3 Centerlines and nodes of inner ear in mini pig

Fig. 4

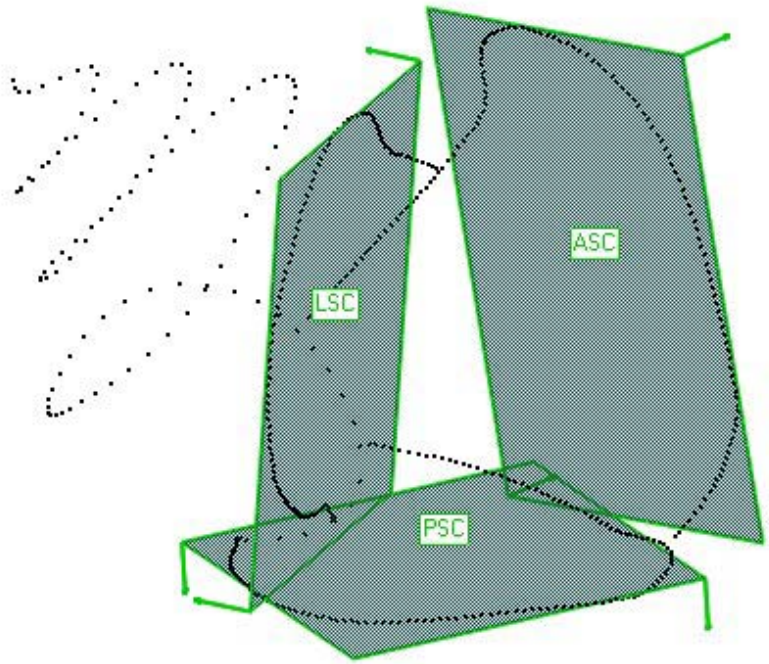

Fig. 4 Illustration of the best fit plane in mini pig model, ASC is the reference plane of anterior semicircular canal, LSC is the reference plane of lateral semicircular canal, PSC is the reference plane of posterior semicircular canal

Fig. 5

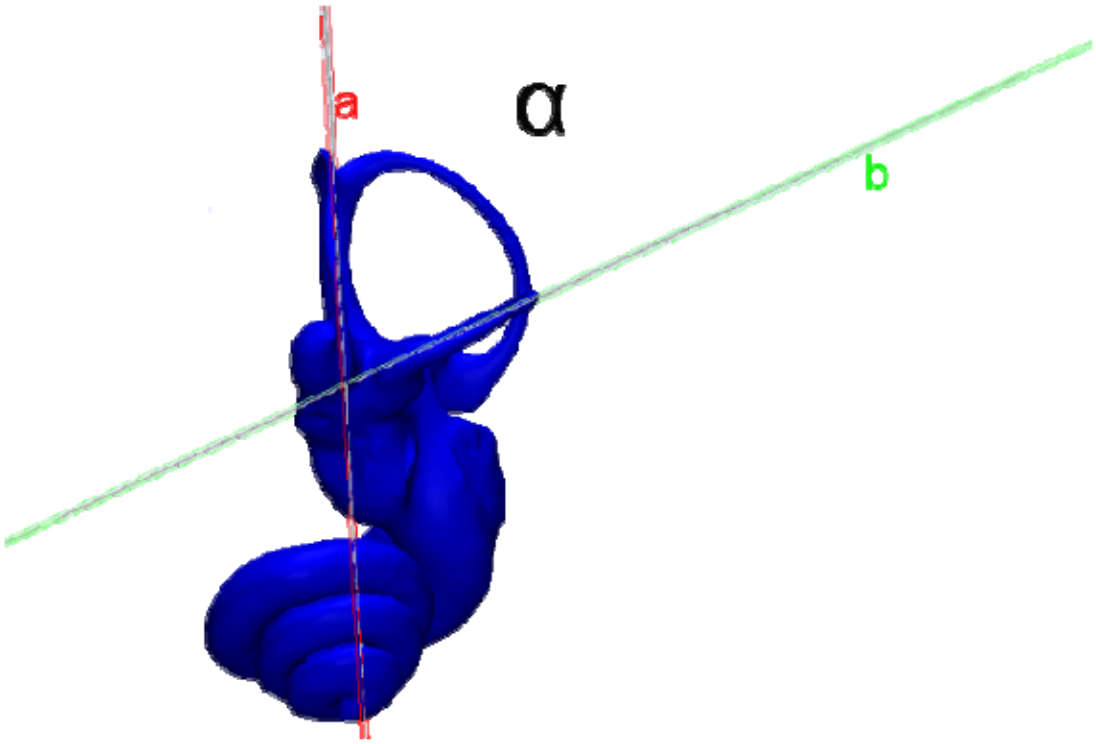

Fig. 5 Illustration of the angle measurement in mini pig model, a: axis of the plane of the anterior semicircular canal; b: axis of the plane of the lateral semicircular canal; α: included angle between a and b

Fig. 6

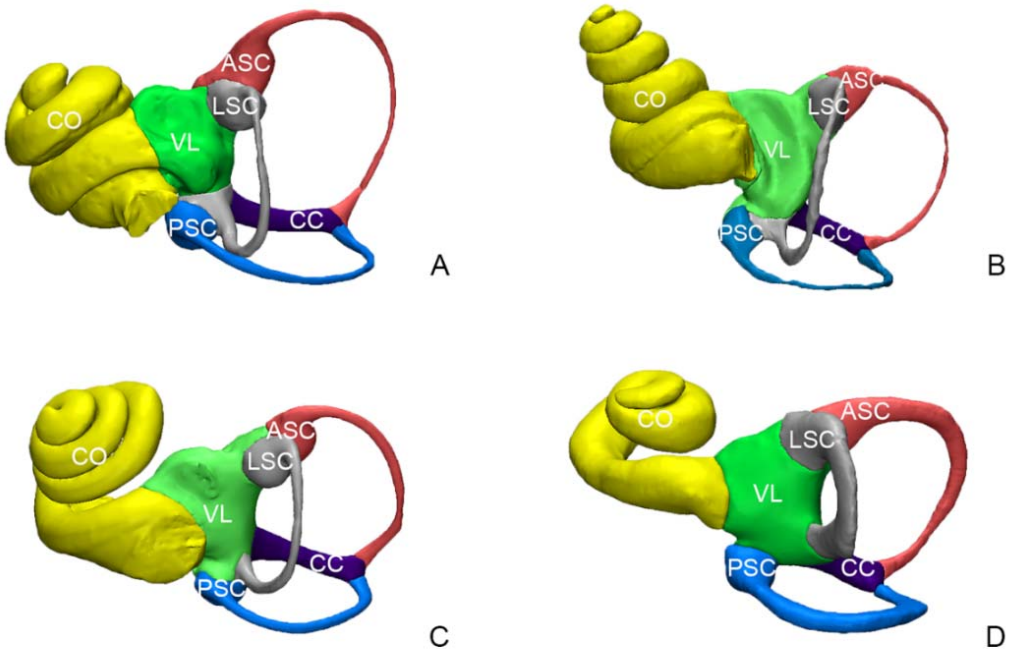

Fig. 6 Illustration of inner ear structure of different mammals.(A: mouse; B: guinea pig; C: mini pig; D: human) CO-cochlea; VL-vestibule; LSC-lateral semicircular canal; ASC-anterior semicircular canal; PSC-posterior semicircular canal; CC-common crus

Fig. 7

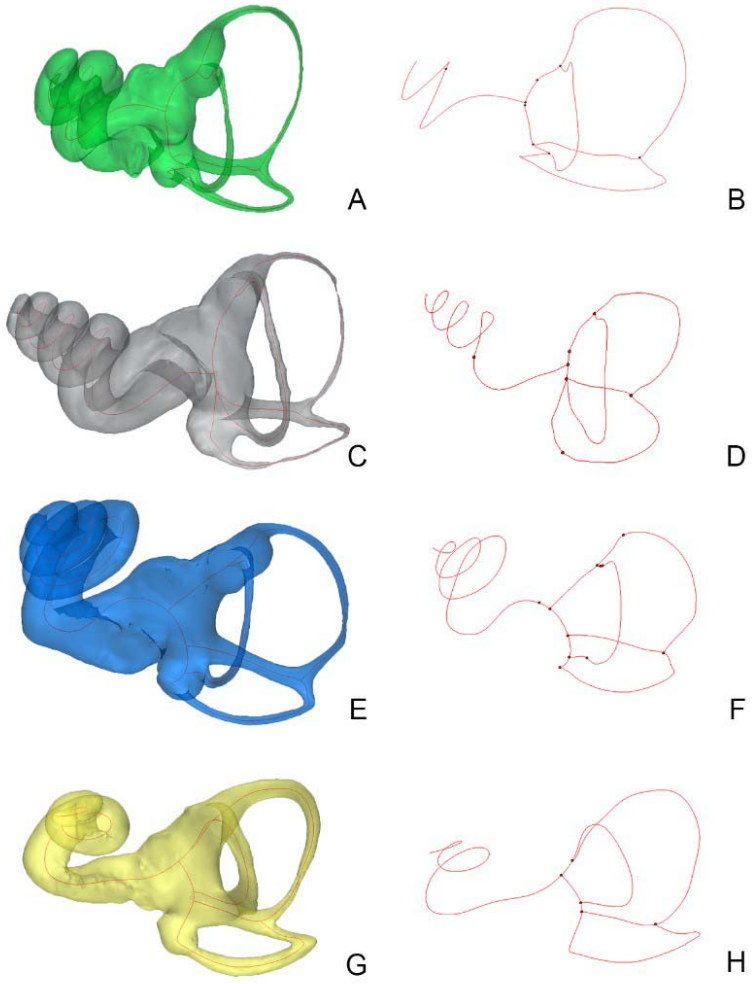

Fig. 7 Centerlines and landmarks in various mammal models. A,B: mouse inner ear model(A) and its centerlines and landmarks(B); C,D: guinea pig inner ear model(C) and its centerlines and landmarks(D); E,F: mini pig inner ear model(E) and its centerline and landmarks(F); G,H: human inner ear model(G) and its centerline and landmarks(H)

Fig. 8

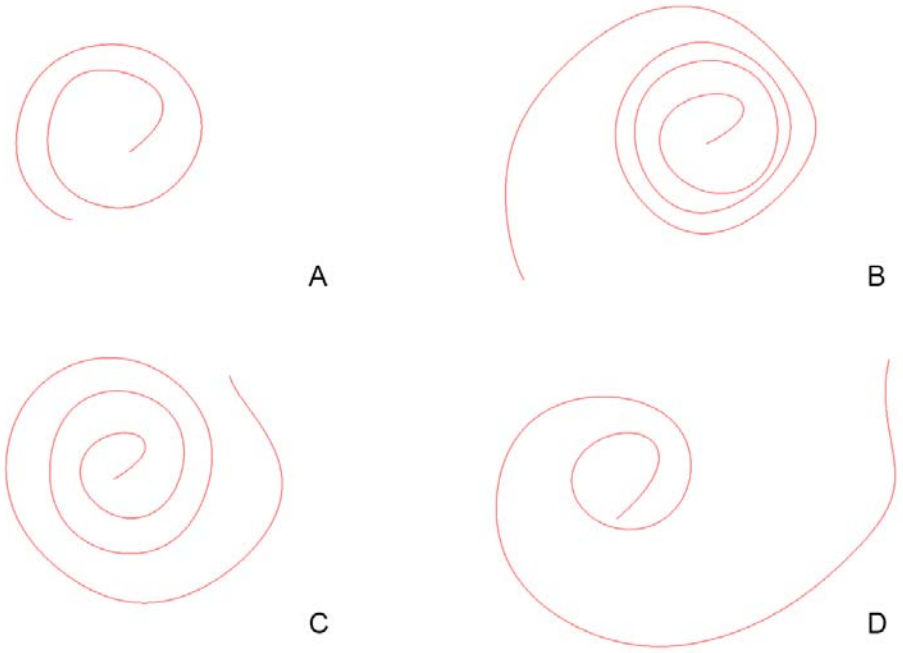

Fig. 8 Cochlear turns of different mammals. A: mouse cochlear; B: guinea pig cochlear; C: pig cochlear; D: human cochlear

Table 1. Length Measurements of Inner Ear

Length (mm)	CO	LSC	ASC	PSC	CC
Mice	6.14±0.36	3.54±0.35	4.28±0.33	3.90±0.35	1.33±0.13
Guinea pigs	17.65±0.53	8.14±0.36	7.60±0.28	7.52±0.69	2.80±0.09
Mini pigs	26.09±1.22	9.72±0.33	9.87±0.67	9.36±0.67	3.98±0.34
Human	24.95	13.26	16.24	16.93	4.15

The value represents mean±SD for the group of mice, guinea pigs and mini pigs

Table 2. Angle Measurements between the Semicircular Canals

Volume (mm^3)	CO	VL	LSC	ASC	PSC	CC
Mice	1.54±0.27	0.55±0.05	0.18±0.05	0.15±0.01	0.14±0.03	0.07±0.01
Guinea pigs	13.68±1.51	7.11±0.89	1.52±0.29	0.79±0.14	0.80±0.20	0.63±0.26
Mini pigs	40.97±5.41	20.53±2.13	3.13±0.92	2.78±0.66	2.41±0.69	1.65±0.30
Human	59.37	46.65	13.70	9.85	12.25	4.28

The value represents mean±SD for the group of mice, guinea pigs and mini pigs

Table 3. Angle Measurements between the Semicircular Canals

	L-A SC (°)	L-P SC (°)	A-P SC (°)	Euclidean distance
Mice	95.84±0.33	97.46±0.80	91.54±2.31	16.10
Guinea pigs	100.77±4.18	83.93±1.88	87.43±2.43	23.13
mini pigs	71.37±4.01	83.45±1.07	86.15±2.15	16.33
Human	81.40	96.24	84.53	0

Abbreviations: L-A SC = angles between lateral and anterior semicircular canals; L-P SC = angles between lateral and posterior semicircular canals; A-P SC = angles between anterior and posterior semicircular canals. The value represents mean±SD for the group of mice, guinea pigs and mini pigs.